8362 J. Med. Chem. 2010, 53, 8362–8367
DOI: 10.1021/jm100993z

Journal of Medicinal Chemistry Article

Novel Small Molecule Inhibitors of MDR *Mycobacterium tuberculosis* by NMR Fragment Screening of Antigen 85C

Christoph Scheich,[§,‡] Vera Puetter,[∥,‡] and Markus Schade*[,†]

[†] *Combinature Biopharm AG, Robert-Roessle-Strasse 10, 13125 Berlin, Germany.* [‡] *Both authors contributed equally.* [§] *Current address: Evotec AG, Robert-Roessle-Strasse 10, 13125 Berlin, Germany.* [∥] *Current address: Bayer Schering Pharma AG, 13342 Berlin, Germany.*

Received August 2, 2010

Protein target-based discovery of novel antibiotics has been largely unsuccessful despite rich genome information. Particularly in need are new antibiotics for tuberculosis, which kills 1.6 million people annually and shows a rapid increase in multiple-drug-resistant cases. By combining fragment-based drug discovery with early whole cell antibacterial screening, we discovered novel ligand-efficient inhibitors of multiple-drug resistant *Mycobacterium tuberculosis* (*Mtb*), which bind to the substrate site of the *Mtb* protein antigen 85C, hitherto unused in *Mtb* chemotherapy.

Introduction

Despite an increasingly high medical need due to multiple drug resistance, antibiotics research has failed to bring new chemical classes of antibiotics to the market for over 25 years and a staggering 40 years for the treatment of tuberculosis (TB[a]).[1,2] Presently *Mycobacterium tuberculosis* (*Mtb*), the causative agent of TB, kills approximately 1.6 million people annually and has infected one-third of the world population, rendering TB the second most lethal infectious disease after HIV/AIDS.[3] With 400 000 new cases annually, multiple-drug resistant TB is emerging rapidly, calling urgently for new anti-TB therapeutics[3]

High-throughput screening of antibacterial targets, typically enzymes, and subsequent in vitro hit optimization led to potent enzyme inhibitors but barely to efficacious bacterial growth inhibitors.[2] Metabolic escape routes and insufficient cell permeability are considered important causes of inactivity. Here we report an improved discovery strategy comprising fragment-based screening to begin with minute highly permeable compounds and early whole cell antibacterial screening to ensure blockage of essential bacterial growth pathways. We validate our approach through the identification of novel anti-tuberculars, a particularly challenging class of antibiotics because of the poorly drug-permeable cell wall shield of mycobacteria.

The mycobacterial cell wall, which is essential for viability and virulence of *Mtb*,[4] consists of three major components forming the mycolyl−arabinogalactan−peptidoglycan (mAGP) complex, among which mycolic acids represent the outermost layer.[5] Mycolic acids are high-molecular-weight α-alkyl-β-hydroxy fatty acids mainly present as trehalose monomycolate (TMM), trehalose dimycolate (TDM or cord factor), and esters of arabinogalactan (Figure 1a). Isoniazid and ethambutol, first line chemotherapeutics for the treatment of TB, inhibit mycobacteria by perturbing the synthesis of mycolic acids and arabinan, respectively. The transfer of mycolates between TMM and TDM is catalyzed by the highly conserved mycolyl transferases antigens 85A, 85B, and 85C (abbreviated Ag85A, -B, and -C).[6]

The cocrystal structures of Ag85A, -B, and -C reveal a catalytic triad formed by Ser124, His260, and Glu228 and an extended hydrophobic trough adjacent to the trehalose site thought to accommodate the mycolyl chain of TMMs and TDMs (Figure 1b).[7,8] Genetic knockout of Ag85A led to the loss of *Mtb* replication in human and mouse macrophages, and knockout of the Ag85C gene reduced the cell-wall linked mycolic acids content by 40%.[9] Covalent chemical inhibition of Ag85A, -B, and -C by the trehalose mimetic 6-azido-6′-deoxytrehalose showed weak in vitro growth inhibition of *Mycobacterium aurum* with a minimum inhibitory concentration (MIC) of 200 μg/mL.[6]

Here we report that novel, noncovalent, fragment-size binders to the substrate site of Ag85C inhibit the growth of *Mtb* and multiple drug-resistant *Mtb* (MDR-*Mtb*). Our *Mtb* inhibitors possess antibacterial ligand efficiencies equal to or better than present anti-tuberculars in clinical phase trials, suggesting that they are attractive chemotypes for further development into novel MDR-*Mtb* chemotherapeutics. Beyond the two chemical classes shown our data further indicate that small molecule inhibition of the Ag85 enzyme family is a promising strategy for combating TB.

Results

Fragment Hit Identification. On the basis of the 3D structural and genetic knockout data, we selected *Mtb* Ag85C as

*To whom correspondence should be addressed. Current address: Pfizer Ltd., PGRD Structural Biology and Biophysics, Sandwich CT13 9NJ, U.K. Phone: +44 1304 642850. Fax: +44-1304-651820. E-mail: markus.schade@pfizer.com.

[a] Abbreviations: Ag85A, -B, and -C, antigens 85A, 85B, and 85C; BEI, binding efficiency index; CSP, chemical shift perturbation; EMB, ethambutol; INH, isoniazid; mAGP, mycolyl−arabinogalactan−peptidoglycan; MDR, multiple drug resistant; MIC, minimum inhibitory concentration; *Msmeg*, *Mycobacterium smegmatis*; *Mtb*, *Mycobacterium tuberculosis*; OTG, *n*-octylthioglucoside; PZA, pyrazinamide; SI, Supporting Information; TB, tuberculosis; TMM, trehalose monomycolate; TDM, trehalose dimycolate; THBT, tetrahydro-1,3-benzothiazole; XDR, extensively drug resistant.

 Published on Web 11/12/2010

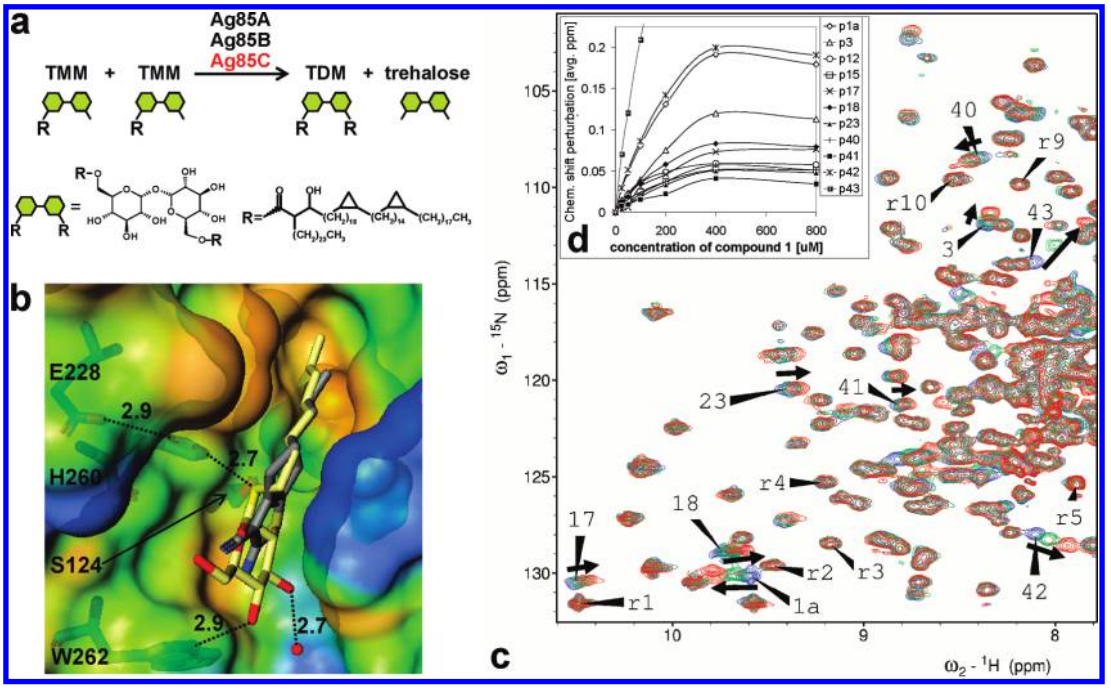

Figure 1. Targeting the Ag85 enzymes. (a) The three enzymes Ag85A, -B, and -C catalyze the mycolyl ("R") transfer from trehalose monomycolate (TMM) to trehalose dimycolate (TDM). (b) The semitransparent surface representation of the cocrystal structure of Ag85C complexed with OTG (C atoms light yellow, PDB code 1va5) shows the glucoside occupying the exact position of the to-be-mycolated trehalose monomer, while the *n*-octyl chain fills a deep extended trough thought to harbor the mycolyl of TMM. The H bonds of the catalytic triad S124, H260, E228 as well as the H bond to W262 are shown as dashed lines with atom distances in Å. A potential pose of **14** (C atoms gray) is shown superimposed on OTG. (c) Overlay of the ^{15}N-HSQC NMR spectra of 50 μM Ag85C alone (blue) and Ag85C in the presence of 100 (green) and 400 μM **1** (red) shows dose-dependent CSPs for the resonances of 11 well-resolved residues (numbered and direction marked by arrows), whereas the resonances of 10 randomly selected reference residues (labeled "r1" to "r10") do not change. (d) Dose-response curves of the 11 residues used to calculate a K_d of 140 ± 30 μM (SD).

a surrogate in vitro screening target for the Ag85 enzyme family. In the absence of robust high-throughput enzymatic assays, we utilized NMR fragment screening by ^{15}N-HSQC NMR spectroscopy, a sensitive direct binding assay for fragments.[10,11] Purified ^{15}N-labeled Ag85C was screened against a diverse library of 5000 synthetic fragments in pools of 16 compounds each. With 0.1% CHAPS detergent present in the assay, which potentially competes with small molecule binding to the hydrophobic active site, we chose stringent screening conditions resulting in a comparatively low hit rate of merely six hits, as defined by three or more resolved chemical shift perturbations (CSPs) above background chemical shift variation (Figure 1c). The cocrystal defined catalytic site ligand *n*-octylthioglucoside (OTG)[8] was used as a positive control, yielding a set of CSPs characteristic for active site binders (Supporting Information (SI) Figure S1).

Unlike literature applications of fragment-based drug discovery, which first affinity-optimize loose fragments in vitro,[11] we immediately subjected the six NMR screening hits to in vitro antibacterial growth assays against *Mycobacterium smegmatis* (*Msmeg*), *E. coli*, and *B. subtilis*. *Msmeg* is a frequently used model strain for *Mtb* because of its markedly lower pathogenicity to humans and faster growth. One of the six compounds, 2-aminocyclohepta[*b*]thiophene-3-carbonitrile (**1**), inhibits the growth of *Msmeg* with an MIC of 50−100 μg/mL but not the growth of *E. coli* or *B. subtilis*, both of which lack the Ag85 gene family and serve as early selectivity filters (SI Figure S2). By contrast, *Msmeg* shares the Ag85A and Ag85C proteins with *Mtb*, both of which show 100% sequence identity in the core catalytic site residues contacting OTG except for one conservative L40M mutation in Ag85A (*Msmeg*).

Fragment Hit Binds to the Catalytic Site. The 30 residues of Ag85C that show CSPs upon addition of **1** yield similar CSPs in the presence of OTG, whereas 10 randomly selected negative control residues remain undisturbed (SI Figure S3), indicating that **1** binds to the active site or a directly adjacent site. Observation of CSP number 17 possessing the characteristic ^{1}H^{15}N chemical shifts of tryptophan NHε atoms is in agreement with **1** binding close to W262 which forms a hydrogen bond with OTG (Figure 1b) and trehalose,[7] although an allosteric CSP effect on a different tryptophan cannot be ruled out. Dose-dependent analysis of the CSPs yielded an equilibrium dissociation constant (K_d) of 140 μM for **1** (Figure 1d), corresponding to K_d- and MIC-based ligand efficiency indices, BEIs of 20 and 18, respectively. K_d- and MIC-based BEIs (defined in SI) allow one to benchmark small molecule inhibitors across a wide range of potencies and guide fragment to lead optimization.[12] Hence, compared with clinically used, non-prodrug *Mtb* antibiotics, such as moxifloxacin, with a MIC-based BEI of 15 against *Mtb*-H37,[13] **1** is a promising ligand-efficient starting structure for further optimization toward an oral anti-tubercular.

Fragment Hit Elaboration. The 192 Da scaffold of **1** was systematically explored for substitutions that increase potency. Because of high sensitivity to small changes in ligand interaction strength, ^{15}N-HSQC NMR spectroscopy was used as the primary assay, followed by whole cell *Msmeg* antibacterial testing. We found that all alternative substituents to the R1 position (defined in Table 1) of **1**, such as acetamide, (4-methyl-1-piperazinyl)methylene, and the cyclic R1/R2 substituent 2-methyloxazin-4-one, were inactive. Similarly the R2 substituents ethyl carboxylate and ethylcarboxamide of **1** were inactive,

Table 1. Ag85C Binding and *Msmeg* Antibacterial Activity of Tetrahydro-1-benzothiophene (THBTP) Analogues[a]

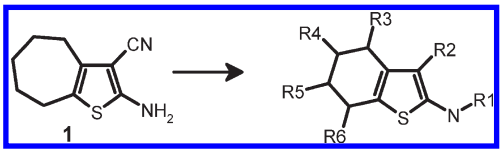

compd	R1	R2	R3	R4	R5	binding to Ag85C [CSP score]	*Msmeg* growth inhibition [MIC, μg/mL]
1[b]	-H	-CN	-H	-H, -H	-H	1.00	64
2	-H	-CN	-H	-H, -H	-H	0.92	nd
3	-CO-CH_3	-CN	-H	-H, -H	-H	i	nd
4	-CO-CH-$(CH_3)_2$	-CN	-H	-H, -H	-H	i	nd
5	-R2	-CONH-C(4-pyridinyl) = R1	-H	-H, -H	-H	i	nd
6	-H	-$CONH_2$	-H	-H, -H	-H	0.61	nd
7	-H	-COO-CH_3	-H	-H, -H	-H	0.69	nd
8	-H	-CONH-CH_2-C_6H_5	-H	-H, -H	-H	i	nd
9	-H	-COO-CH_2-CH_3	-CH_3	-H, -H	-H	0.54	nd
10[c]	-H	-CN	-H	-CH_3, -CH_3	-H	i	nd
11[c]	-H	-CN	-H	-CH_3, -CH_2-CH_3	-H	i	nd
12	-H	-CN	-H	-H, -H	-CH_3	1.00	nd
13	-H	-CN	-H	-H, -H	-CH_2-CH_3	1.27	32
14	-H	-CN	-H	-H, -H	-CH_2-CH_2-CH_3	0.78	16
15	-H	-$CONH_2$	-H	-H, -H	-CH_3	0.23	> 32
16	-H	-$CONH_2$	-H	-H, -H	-CH_2-CH_3	1.05	64
17	-H	-$CONH_2$	-H	-H, -H	-CH_2-CH_2-CH_3	0.76	64
18a	-H	-CN	-H	-H, -H	-C-$(CH_3)_3$	i	nd
18b[d]	-H	-CN	-H	-H, -H	-CH_2-CH_3	i	nd
18c[e]	-H	-CN	-CH_2-CH_2-R6	-H, -H	-H	i	nd

[a] The THBTP scaffold is chemically similar to the original hit **1**. i = inactive. nd = not determined. CSP score is defined in Experiment Section. If not otherwise defined, unsaturated valencies are hydrogen. [b] Cyclohepta[*b*]thiophene scaffold. [c] 4,7-Dihydro-5*H*-thieno[2,3-*c*]pyran scaffold. [d] 4,7-Dihydro-5*H*-thieno[2,3-*c*]pyridine scaffold. [e] 3-Thia-1-azatricyclo[5.2.2.0-2,6-]undeca-2(6),4-diene scaffold (SI Figure S6).

although insufficient solubility of the last two analogues may have contributed to their inactivity.

Searching for additional analogues, we allowed the cyclohepta[*b*]thiophene scaffold of **1** to shrink by one carbon to cyclohexa[*b*]thiophene (**2**), which was almost as active in our NMR assay as **1**, as evidenced by a CSP score of 0.92 (Table 1). The CSP score is the ratio of observed CSPs between an analogue and **1**, i.e., CSP scores smaller than 1, equal to 1, and larger than 1 represent Ag85C binding activities smaller than, equal to, and larger than that of **1**, respectively. In addition to the CSP readout, all analogues were checked for solubility in our assay by recording gated 1D ^{1}H NMR spectra.

R5 Alkyl Substituents Improve Activity. As before, all substitutions at the R1 position of **2** that were investigated, such as acetamide (**3**), 2-methylpropanamide (**4**), and the cyclic R1/R2 substituent 6-pyridinylpyrimidin-4-one (**5**), were inactive. However, small substitutions to the R2 position, such carboxamide (**6**) and methylcarboxylate (**7**), showed binding, albeit with lower affinity than **1**. Substitution of positions R3, R4, and R6 in **2** again resulted in inactive or weaker binders. Elaboration at the R5 position, however, resulted in equal or elevated binding strength in the NMR assay. Methyl, ethyl, and *n*-propyl substitutions at R5 were tolerated in the presence of carbonitrile (**12**, **13**, **14**) and carboxamide (**15**, **16**, **17**) at the R2 position, of which the carbonitrile analogues consistently showed higher affinities. In contrast a bulky tertiary butyl at R5 (**18a**) led to inactivity, and introduction of nitrogen at the R5 branch site along with an ethyl substituent at R5 (**18b**) yielded CSPs at different resonances of Ag85C but no activity at the characteristic CSPs of OTG. Similarly insertion of nitrogen at the R6 branch position and linking it with an ethylene to the R3 branch position (**18c**) resulted in loss of Ag85C binding.

Testing the five binding active R5 analogues **13**−**17** for *Msmeg* growth inhibition revealed improved MICs of 32 and 16 μg/mL for **13** and **14**, respectively. Compared with **1**, this equals 2- and 4-fold higher antibacterial potencies and *Msmeg* MIC-based BEIs of 19 for **13** and **14**. The lower CSP score of **14** with respect to **13** and **1** is probably due to the limited solubility of **14** in the NMR assay causing a lower effective concentration in the assay.

R5 Substituted Benzothiazoles Are Alternative Inhibitors. To further expand our synthetic hit-to-lead options, we explored 1,3-benzothiazole and tetrahydro-1,3-benzothiazole (THBT) as alternative scaffolds (SI Table S4 and Figure S5), in which the R2 carbonitrile is shortened to a ring nitrogen. The R5 methyl substituted THBT analogue (**19**) is active in the NMR binding assay, but its CSP score of 0.69 indicates lower affinity than the corresponding R2 carbonitrile analogue **12**. Surprisingly the R5 dimethyl and R3 oxo substituted THBT (**20**) shows a CSP pattern indicative of binding to another site of Ag85C and no antibacterial activity at 64 μg/mL or below. This suggests that the second methyl group and the cyclic keto function cannot be accommodated in the given binding geometry and is in line with the inactivity of the R5 tertiary butyl analogue **18a**.

The R5 methyl substituted benzothiazole (**21**) binds to Ag85C more tightly than the THBT counterpart **19** but is still weaker than **12**. Extension of the R5 substituent to propoxy (**22**) increases binding affinity marginally by 0.03 CSP-score points but antibacterial activity substantially,

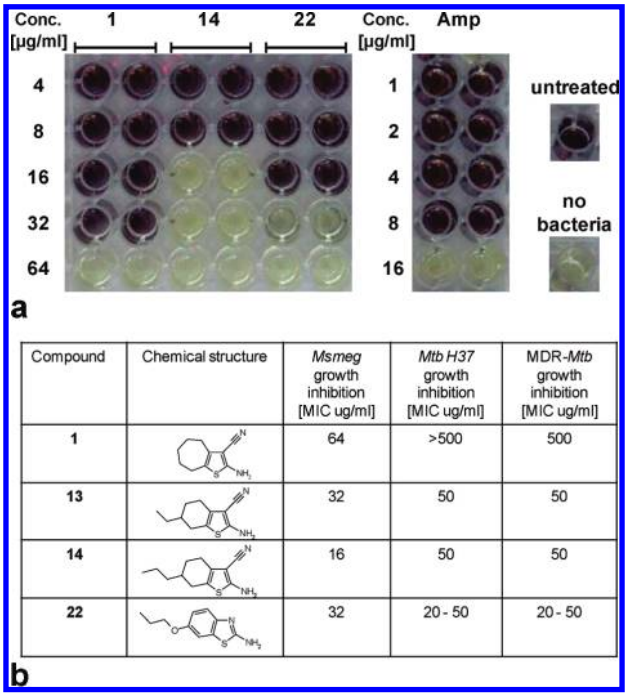

Compound	Chemical structure	*Msmeg* growth inhibition [MIC ug/ml]	*Mtb H37* growth inhibition [MIC ug/ml]	MDR-*Mtb* growth inhibition [MIC ug/ml]
1		64	>500	500
13		32	50	50
14		16	50	50
22		32	20 - 50	20 - 50

b

Figure 2. *Msmeg*, *Mtb*-H37, and MDR-*Mtb* in vitro growth inhibition of improved analogues. (a) No visually detectable growth of *Msmeg* is observed when 64, 16, and 32 μg/mL **1**, **14**, and **22**, respectively, are added to the bacterial growth medium. The reference antibiotic ampicillin (Amp) inhibits *Msmeg* growth at 16 μg/mL, as published previously.[25] Growth medium with (labeled "untreated") and without bacteria inoculum (labeled "no bacteria") is colored black and pale yellow, respectively. (b) Chemical structures and antimycobacterial activities of the key compounds **1**, **13**, **14**, and **22**.

resulting in a 2-fold lower *Msmeg* MIC than **1**. By contrast more polar, extended R5 substituents, such as acetamide (**23**) and *sec*-butylcarboxamide (**24**), did not bind, suggesting a preference for lipophilic unbranched substituents at R5. Also nitro substituents at the R3 position (**25**, **26**) led to inactivity. By contrast, a R4 chloro along with a R5 methoxy (**27**) was tolerated, whereas a larger R4 acetamide in conjunction with a R5 methyl (**28**) showed no binding. Taken together, benzothiazole analogues bind to Ag85C, and the best analogue **22** shows improved solubility and *Msmeg* antibacterial activity with a BEI of 18.

Inhibition of *Mtb*-H37 and MDR-*Mtb*. On the basis of this structure−activity relationship data, we prioritized **13**, **14**, and **22** for antibacterial assays with pathogenic *Mtb*-H37 and MDR-*Mtb*. In good correlation with the activities against *Msmeg*, **13**, **14**, and **22** inhibited the growth of *Mtb*-H37 with MICs of 50, 50, and 20−50 μg/mL in the radiometric BACTEC 460 assay, respectively (Figure 2b). Identical MICs were observed against the isoniazid-resistant MDR-*Mtb* strain 2745/09. Equal antibacterial activity against *Mtb*-H37 and MDR-*Mtb* is in agreement with these compounds blocking cell wall biosynthesis via the antigen 85 complex, which is downstream of inhA, the mycolic acid biosynthesis enzyme blocked by isoniazid,[1] although alternative modes of action cannot be ruled out. The starting fragment **1** yielded an 8-fold higher MIC against MDR-*Mtb* than *Msmeg* and was inactive against *Mtb*-H37 at the top 500 μg/mL concentration tested, suggesting that the colorimetric *Msmeg* assay is more sensitive to weak fragments.

Discussion

Following the therapeutic success of the exceptionally low M_w first-line TB chemotherapeutics isoniazid (INH), pyrazinamide (PZA), and ethambutol (EMB), we chose fragment based drug discovery to search for similarly low M_w inhibitors of the cell-wall biosynthesis enzymes Ag85. By using robust protein-observed NMR screening, we identified six novel low M_w binders to the surrogate family member Ag85C. Alerted by the numerous potent in vitro enzyme inhibitors that were later found to be inactive against whole bacteria,[2] we immediately filtered the six Ag85C binders for bacterial growth inhibition and selectivity for mycobacteria. Only one of the six in vitro Ag85C binders passed this stringent antibacterial activity filter, allowing us to focus on fragment hit **1** early and to substantiate SAR exploration with *Msmeg* MIC values. By contrast, 5-*S*-octyl-5-thio-D-arabinofuranosides, designed to mimic the mycolyl−arabinogalactan product of Ag85 enzymes, show indiscriminative inhibition of *Msmeg* and *B. subtilis* growth, which suggests an off-target mode-of-action.[14] Ligand efficiency analysis underscored that **1** is an excellent starting scaffold with an in vitro binding or K_d-based efficiency index BEI of 20, which is comparable with hinge binding protein kinase inhibitors.[15]

Next we confirmed by NMR that **1** binds to the same site as the cocrystal defined ligand OTG or to an immediately adjacent site in the catalytic substrate trough of Ag85C. Therefore, **1** is expected to competitively inhibit the mycolyl transferase activity of Ag85C and also of Ag85A and Ag85B because of the 100% sequence and 3D structure conservation of the core OTG contacting residues. Simultaneous blockage of Ag85A, -B, and -C by RNA antisense inhibited the growth of *Mtb* by 2 log units in culture broth,[16] whereas genetic knockout of either Ag85A or -C alone did not. Hence, pan-Ag85 inhibition by **1** is in agreement with the RNA antisense data and the pan-Ag85 effects of 6-azido-6′-deoxytrehalose on *M. Aurum* growth, whereas single gene blockage is not expected to fully restrict *Mtb* growth.

Since cocrystallization and soaking experiments to obtain a high resolution structure of **1** complexed with Ag85C yielded only apo-structures but no unambiguous electron density for **1**, fragment elaboration was performed by systematically testing available analogues of **1**. We explored substitution of the synthetically accessible positions R1−R6 of **1** and consistently found for the two related scaffolds cyclohexa-[*b*]thiophene and benzothiazole that unbranched alkyl or heteroatom substituted alkyl side chains at R5 increase both Ag85C binding activity in the NMR assay and antibacterial activity against *Msmeg*. By contrast, all R1, R4, or R6 substituted cyclohexa- or cyclohepta[*b*]thiophenes except for **27** were inactive, suggesting a tight SAR as expected for the narrow substrate pocket of Ag85C. Replacement of the R5 ring carbon of **13** with a basic nitrogen in **18b**, which increases aqueous solubility, led to inactivity. Similarly, polar amide and retroamide substituents were not tolerated at the R5 position of the benzothiazoles **23** and **24**. This preference for lean, hydrophobic alkyl or heteroalkyl chains at R5 is reminiscent of the octylthio chain of OTG and the mycolyl chains of TMM and TDM and leads us to hypothesize that the R5 substituents of **14** and **22** occupy the mycolyl channel of Ag85C, while the 2-aminothiophene or 2-aminothiazole maps to the trehalose recognition site of Ag85C (SI Figure S7). According to this binding model, the mycolyl channel holds substantial unoccupied space for further elaboration along

the R5 position beyond the propoxy chain of **22** and opportunities for designing in additional polarity along the R2 position of **14** (SI Figure S8).

Comparison of antibacterial ligand efficiency indices, BEIs, indicate that **14** and **22** are excellent starting structures for further fragment elaboration. With BEIs against *Msmeg* of 18, **14** and **22** are twice as ligand efficient as the covalent Ag85C inhibitor 6-azido-6-deoxytrehalose and the most active noncovalent trehalose mimetic with BEI against *M. aurum* of 9[6,17] and the most active synthetic phosphonate and sulfonate inhibitors of Ag85C, designed to mimic the enzyme transition state, with *Msmeg* BEI of 9.[18,19] Against *Mtb*-H37 and MDR-*Mtb*, **14** and **22** show almost identical BEIs of 17 and 18, respectively, which compare very favorably with the present anti-TB clinical phase III candidate moxifloxacin and the phase II candidates PA-824, OPC-67683, and TMC207 with *Mtb*-H37 BEIs of 15, 17, 14, and 13, respectively.[13,20,21] The first-line anti-tubercular ethambutol possesses a higher *Mtb*-H37 BEI of 25, but its attractiveness is compromised by a suboptimal *Mtb*-H37 MIC of 2 μg/mL.[20] Hence chemical optimization of **14** or **22** may yield antituberculars of better potency than ethambutol and better ligand efficiency than current clinical candidates.

Since **14** and **22** show equal potency against *Mtb*-H37 and MDR-*Mtb*, **14** and **22** derived anti-tuberculars could improve present TB combination therapy because cross-resistance with isoniazid and rifampin is not expected. Furthermore by addressing a yet unused target in clinical and field TB chemotherapy, Ag85 inhibitors may also favorably supplement future anti-TB drug cocktails by killing latent *Mtb* and extensively drug-resistant (XDR) *Mtb* more quickly and more thoroughly. As **14** and **22** are readily available through one-step synthetic reactions,[22,23] low cost-of-goods production and broad distribution to patients in third world countries might be achievable.

In conclusion, this work establishes the antigen 85 complex as a new chemotherapeutic target for MDR-*Mtb* infections and discloses highly ligand-efficient inhibitors. In addition our chemical inhibitors may be valuable tools for the investigation of pan-Ag85 blockage in *Mtb* biology, delivering phenotypes not obtainable by single gene knockouts.

Experimental Section

Protein Production. ^{15}N-Labeled *Mtb* Ag85C protein was produced by cloning the synthetic gene of the cocrystal defined construct[24] into the vector pET20b and expressing it with a C-terminal $(His)_6$-tag in *E. coli* Bl21(DE3)pLysS in M9 minimal medium enriched with 1 g/L ^{15}N-ammonium chloride and 0.4% glucose at 17 C. Cells were disrupted by sonication and French pressing in 50 mM Tris, pH 8.0, 500 mM NaCl, 1 mM DTT, 40 mM $MgCl_2$, 5 μg/L DNase, Roche Complete, and PEFABloc protease inhibitor mix. The soluble fraction was loaded on a Ni metal chelating column, washed with 50 mM Tris, pH 8.0, 500 mM NaCl, 20 mM imidazole, 0.2 mM DTT, and eluted with 50 mM Tris, pH 7.5, 250 mM NaCl, 250 mM imidazole, 0.5 mM DTT. The eluate was loaded on a phenyl FF hydrophobic interaction chromatography column, washed, and eluted with 10 mM Tris, pH 8.6, 1 mM DTT, 1 mM EDTA. The eluate was concentrated and changed into 5 mM Na citrate, pH 6.0, 1 mM DTT, 0.1% CHAPS by using a Hi Prep 26/10 desalting column.

NMR Fragment Screen and Binding Assay. NMR fragment screening was performed with 30 μM ^{15}N-labeled Ag85C in the presence of a mixture of 16 compounds at 250 μM each in 5 mM Na citrate, pH 6, 1 mM DTT, 0.1% CHAPS, and 5% DMSO-d_6 by using 2D ^{15}N-HSQC NMR spectroscopy (600 MHz spectrometer, 64 scans, 96 or 128 indirect points). Hits in mixtures were confirmed by single compound experiments. Fragment hit elaboration assays were carried out as single compound assays with 30 or 50 μM protein and 100, 250, or 1000 μM compound under otherwise identical conditions. Chemical shift perturbations (CSPs) of backbone amide resonances were calculated by averaging the ^{1}H and ^{15}N chemical shift differences, Δ^1H and Δ^{15}N, as follows: $CSP = [(\Delta^1H)^2 + (0.2)(\Delta^{15}N)^2]^{0.5}$.

The K_d of **1** was obtained by fitting each binding curve with 11 well-resolved CSPs against the "A + B = AB" law of mass action and averaging the individual K_d values.

The relative CSP scores in the table in SI were calculated by averaging the CSPs of seven resonances, which are well-resolved across the spectra of all compounds assayed. The average CSP of a test compound was divided by the corresponding average CSP of **1** at identical compound concentrations to yield the final CSP score. The single concentration point CSP score is not strictly equivalent to a thermodynamic affinity parameter, such as K_d. In addition to compound binding dynamic processes can also perturb the Δ^1H and Δ^{15}N values, although resonances that titrated well in the K_d determination of **1** were used.

Compounds were prepared as prediluted 20−50 mM DMSO-d_6 stock solutions and mixed with the aqueous protein/buffer solution.

Antibacterial in Vitro Assays. See SI.

Acknowledgment. We thank Sabine Rüsch-Gerdes (National Reference Center for Mycobacteria, Borstel, Germany) for *Mtb*-H37 and MDR-*Mtb* assay support, Antje Starke and Jan Kahmann (Evotec AG, Germany) and Peter Schmieder (FMP, Berlin, Germany) for their assistance with NMR experiments, Melanie Meiworm (Evotec AG, Germany) for her support in protein production, and Yvette Roske and Udo Heinemann (MDC, Berlin, Germany) for their great effort in Ag85C crystallography. Further we thank Thulasi Warrier, Ali Nasser Eddine, and Stefan Kaufmann (MPI Infection Biology, Berlin, Germany) for guidance in *Mtb* biology and are grateful for the financial support by the German Federal Ministry of Research (BMBF) Grant 0312992K.

Supporting Information Available: NMR binding site and antibacterial assay results for the above-mentioned compounds, definition of BEI, and experimental methods. This material is available free of charge via the Internet at http://pubs.acs.org.

References

(1) Zhang, Y.; Post-Martens, K.; Denkin, S. New drug candidates and therapeutic targets for tuberculosis therapy. *Drug Discovery Today* **2006**, *11*, 21–27.
(2) Payne, D. J.; Gwynn, M. N.; Holmes, D. J.; Pompliano, D. L. Drugs for bad bugs: confronting the challenges of antibacterial discovery. *Nat. Rev. Drug Discovery* **2007**, *6*, 29–40.
(3) Young, D. B.; Perkins, M. D.; Duncan, K.; Barry, C. E., 3rd. Confronting the scientific obstacles to global control of tuberculosis. *J. Clin. Invest.* **2008**, *118*, 1255–1265.
(4) Kremer, L.; Dover, L. G.; Carrere, S.; Nampoothiri, K. M.; Lesjean, S.; Brown, A. K.; Brennan, P. J.; Minnikin, D. E.; Locht, C.; Besra, G. S. Mycolic acid biosynthesis and enzymic characterization of the beta-ketoacyl-ACP synthase A-condensing enzyme from *Mycobacterium tuberculosis*. *Biochem. J.* **2002**, *364*, 423–430.
(5) Brennan, P. J.; Nikaido, H. The envelope of mycobacteria. *Annu. Rev. Biochem.* **1995**, *64*, 29–63.
(6) Belisle, J. T.; Vissa, V. D.; Sievert, T.; Takayama, K.; Brennan, P. J.; Besra, G. S. Role of the major antigen of *Mycobacterium tuberculosis* in cell wall biogenesis. *Science* **1997**, *276*, 1420–1422.
(7) Anderson, D. H.; Harth, G.; Horwitz, M. A.; Eisenberg, D. An interfacial mechanism and a class of inhibitors inferred from two crystal structures of the *Mycobacterium tuberculosis* 30 kDa major secretory protein (antigen 85B), a mycolyl transferase. *J. Mol. Biol.* **2001**, *307*, 671–681.
(8) Ronning, D. R.; Vissa, V.; Besra, G. S.; Belisle, J. T.; Sacchettini, J. C. *Mycobacterium tuberculosis* antigen 85A and 85C structures

confirm binding orientation and conserved substrate specificity. *J. Biol. Chem.* **2004**, *279*, 36771–36777.
(9) Jackson, M.; Raynaud, C.; Laneelle, M. A.; Guilhot, C.; Laurent-Winter, C.; Ensergueix, D.; Gicquel, B.; Daffe, M. Inactivation of the antigen 85C gene profoundly affects the mycolate content and alters the permeability of the *Mycobacterium tuberculosis* cell envelope. *Mol. Microbiol.* **1999**, *31*, 1573–1587.
(10) Schade, M. NMR fragment screening: advantages and applications. *IDrugs* **2006**, *9*, 110–113.
(11) Hajduk, P. J.; Greer, J. A decade of fragment-based drug design: strategic advances and lessons learned. *Nat. Rev. Drug Discovery* **2007**, *6*, 211–219.
(12) Abad-Zapatero, C.; Metz, J. T. Ligand efficiency indices as guideposts for drug discovery. *Drug Discovery Today* **2005**, *10*, 464–469.
(13) Shandil, R. K.; Jayaram, R.; Kaur, P.; Gaonkar, S.; Suresh, B. L.; Mahesh, B. N.; Jayashree, R.; Nandi, V.; Bharath, S.; Balasubramanian, V. Moxifloxacin, ofloxacin, sparfloxacin, and ciprofloxacin against *Mycobacterium tuberculosis*: evaluation of in vitro and pharmacodynamic indices that best predict in vivo efficacy. *Antimicrob. Agents Chemother.* **2007**, *51*, 576–582.
(14) Sanki, A. K.; Boucau, J.; Srivastava, P.; Adams, S. S.; Ronning, D. R.; Sucheck, S. J. Synthesis of methyl 5-*S*-alkyl-5-thio-D-arabinofuranosides and evaluation of their antimycobacterial activity. *Bioorg. Med. Chem.* **2008**, *16*, 5672–5682.
(15) Hajduk, P. J. Fragment-based drug design: how big is too big? *J. Med. Chem.* **2006**, *49*, 6972–6976.
(16) Harth, G.; Horwitz, M. A.; Tabatadze, D.; Zamecnik, P. C. Targeting the *Mycobacterium tuberculosis* 30/32-kDa mycolyl transferase complex as a therapeutic strategy against tuberculosis: proof of principle by using antisense technology. *Proc. Natl. Acad. Sci. U.S.A.* **2002**, *99*, 15614–15619.
(17) Rose, J. D.; Maddry, J. A.; Comber, R. N.; Suling, W. J.; Wilson, L. N.; Reynolds, R. C. Synthesis and biological evaluation of trehalose analogs as potential inhibitors of mycobacterial cell wall biosynthesis. *Carbohydr. Res.* **2002**, *337*, 105–120.
(18) Gobec, S.; Plantan, I.; Mravljak, J.; Svajger, U.; Wilson, R. A.; Besra, G. S.; Soares, S. L.; Appelberg, R.; Kikelj, D. Design, synthesis, biochemical evaluation and antimycobacterial action of phosphonate inhibitors of antigen 85C, a crucial enzyme involved in biosynthesis of the mycobacterial cell wall. *Eur. J. Med. Chem.* **2007**, *42*, 54–63.
(19) Kovac, A.; Wilson, R. A.; Besra, G. S.; Filipic, M.; Kikelj, D.; Gobec, S. New lipophilic phthalimido- and 3-phenoxybenzyl sulfonates: inhibition of antigen 85C mycolyltransferase activity and cytotoxicity. *J. Enzyme Inhib. Med. Chem.* **2006**, *21*, 391–397.
(20) Protopopova, M.; Hanrahan, C.; Nikonenko, B.; Samala, R.; Chen, P.; Gearhart, J.; Einck, L.; Nacy, C. A. Identification of a new antitubercular drug candidate, SQ109, from a combinatorial library of 1,2-ethylenediamines. *J. Antimicrob. Chemother.* **2005**, *56*, 968–974.
(21) Matsumoto, M.; Hashizume, H.; Tomishige, T.; Kawasaki, M.; Tsubouchi, H.; Sasaki, H.; Shimokawa, Y.; Komatsu, M. OPC-67683, a nitro-dihydro-imidazooxazole derivative with promising action against tuberculosis in vitro and in mice. *PLoS Med.* **2006**, *3*, 2131–2144.
(22) Sridhar, M.; Rao, R. M.; Baba, N. H. K.; Kumbhare, R. M. Microwave accelerated Gewald reaction: synthesis of 2-aminothiophenes. *Tetrahedron Lett.* **2007**, *48*, 3171–3172.
(23) Jimonet, P.; Audiau, F.; Barreau, M.; Blanchard, J. C.; Boireau, A.; Bour, Y.; Coleno, M. A.; Doble, A.; Doerflinger, G.; Huu, C. D.; Donat, M. H.; Duchesne, J. M.; Ganil, P.; Gueremy, C.; Honor, E.; Just, B.; Kerphirique, R.; Gontier, S.; Hubert, P.; Laduron, P. M.; Le Blevec, J.; Meunier, M.; Miquet, J. M.; Nemecek, C.; Mignani, S.; et al. Riluzole series. Synthesis and in vivo "antiglutamate" activity of 6-substituted-2-benzothiazolamines and 3-substituted-2-imino-benzothiazolines. *J. Med. Chem.* **1999**, *42*, 2828–2843.
(24) Ronning, D. R.; Klabunde, T.; Besra, G. S.; Vissa, V. D.; Belisle, J. T.; Sacchettini, J. C. Crystal structure of the secreted form of antigen 85C reveals potential targets for mycobacterial drugs and vaccines. *Nat. Struct. Biol.* **2000**, *7*, 141–146.
(25) Stephan, J.; Mailaender, C.; Etienne, G.; Daffe, M.; Niederweis, M. Multidrug resistance of a porin deletion mutant of *Mycobacterium smegmatis*. *Antimicrob. Agents Chemother.* **2004**, *48*, 4163–4170.